

Generalized Reference Signals Design for Integrated Communication and Sensing with High-Resolution Algorithms

Rui Zhang
Department of Electrical
Engineering
University at Buffalo
Buffalo, NY, USA
rzhang45@buffalo.edu

Shawn Tsai
Advanced Comm. Technology
Comm. System Design
MediaTek USA Inc.
San Diego, CA, USA
shawn.tsai@mediatek.com

Jiaying Ren
Advanced Comm. Technology
Comm. System Design
MediaTek USA Inc.
San Diego, CA, USA
jiaying.ren@mediatek.com

Oliver Sun
Advanced Comm. Technology
Comm. System Design
MediaTek
Hsinchu, Taiwan, R.O.C
oliver.sun@mediatek.com

Abstract— Delay and Doppler ambiguities of comb reference signal patterns are investigated through time delay and Doppler shift detection using high-resolution sensing algorithms. Necessary conditions of designing comb RS pattern and synthesizing different reference signal patterns in general are derived under the goal of eliminating side peaks and preserving the best achievable ambiguity performance of OFDM signals for target detection.

Keywords—Integrated communication and sensing, reference signal, 6G

I. INTRODUCTION

In recent years there is a growing interest in integrated communication and sensing (ICAS) for the 5th generation advanced (5G-A) and the upcoming 6th generation (6G) mobile communication systems [1, 2]. It is envisioned that wireless networks will evolve to incorporate additional sensing functions to support emerging applications at a low cost. The next-generation wireless system can share waveform, reference signal, and most hardware components with enablers for sensing. There have been extensive research efforts of waveforms and reference signals (RSs) for ICAS. Orthogonal Frequency Division Multiplexing (OFDM), widely adopted in current cellular and Wi-Fi networks, has been investigated in radar sensing under various algorithms, including matched filter, maximum likelihood detection, estimation of signal parameters via rotational invariance technique (ESPRIT) [3-5], etc. For bi-static sensing where data payload is not known, RS is the most straightforward radio resource for the sensing receiver to estimate delays and Doppler shifts caused by targets. In [6,7], LTE RSs and positioning reference signal (PRS) have been analyzed for radar sensing. A joint reference signal design and power optimization is proposed for energy-efficient 5G vehicle-to-everything (V2X) ICAS [8].

There are a few types of RS in 5G New Radio (NR) system: Demodulation RS (DMRS), channel state information RS (CSI-RS), tracking RS (TRS), phase tracking RS (PTRS), and PRS [9]. Among them, multiple comb RS symbols with a cycle of staggering offsets within the coherent processing interval (CPI) is adopted in 5G PRS to preserve the maximum unambiguous delay within one effective OFDM symbol length [9]. However, 5G PRS was optimized only for delay estimation with a special design in the staggering offset sequence. Therefore, extra aspects derived from general sensing criteria require another look at other possibilities. Specifically, with Doppler shift adding to the estimated variables, ambiguities arise in the two-

dimensional delay-and-Doppler plane. In general, there would be trade-offs between time delay or Doppler shift ambiguities and time delay or Doppler shift resolution in RS design. We found that, by designing appropriate staggering offsets over multiple symbols and spacing between resource elements (REs) in the time and frequency domain, the ambiguity performance in both time delay and Doppler shift domain can be greatly improved when a high-resolution type of sensing algorithms, such as iterative adaptive approach (IAA) [10] and 2D Multiple Signal Classification (MUSIC) [11,12], is adopted. Also, synthesis of new, generalized RS patterns could achieve the best ambiguity performance when a set of necessary conditions is satisfied.

II. COMB RS PATTERNS WITH UNIFORM SYMBOL SPACING

We characterize the comb RS patterns with uniform symbol spacing as follows. As shown in Fig. 1, let $S_{sub} (\geq 2, \text{unit in subcarrier numbers})$ be the spacing of the RS resource elements (REs) in frequency domain for the comb structure, $S_{sym} (\geq 1, \text{unit in symbol numbers})$ be the spacing of the RS symbols in the time domain, $F_m (\in \mathbb{Z}, \text{unit in subcarrier numbers})$ be the staggering offset (or RE offset) in the frequency domain of the m -th RS symbol, and M and N be the number of RS symbols and number of RS REs, respectively. The RS pattern can be tuned by S_{sub} , S_{sym} , F_m , M and N . Fig. 1 shows one example with $S_{sub} = 4$, $S_{sym} = 2$, $\{F_0, F_1\} = \{0, 2\}$, $M = 2$, and $N = 3$.

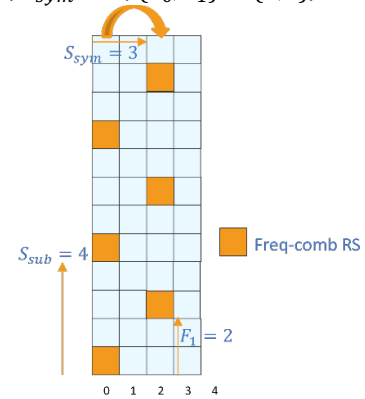


Figure 1. Illustration of general comb RS pattern.

The comb structure has several benefits. First, it boosts energy per RE (EPRE) for better coverage, compared to full symbol TDM. Second it can maximize the delay resolution by spanning across the entire channel bandwidth, giving advantage

over sub-band FDM. Third, it enables different gNB PRS multiplexing or allows for data REs insertion when EPRE is not a constraint. With a fixed number of REs for RS, increasing S_{sub} (occupied bandwidth) and S_{sym} (time duration) enhance the range (delay) resolution and the velocity (Doppler) resolution. In this section, we will focus on ambiguity performance analysis of such RS patterns with uniform symbol spacing when high-resolution sensing algorithms are adopted.

A. System Model and Algorithm Principles

To simultaneously detect the target velocity and range, here we leverage 2D MUSIC and 2D IAA as examples of high-resolution sensing algorithms. Let the RS signal matrix of the 1st to the M -th RS symbol before IFFT in one snapshot at the transmitter side be:

$$\mathbf{F}_{Tx} = \begin{pmatrix} c_{F_0,0} & \cdots & c_{F_{M-1},(M-1)S_{sym}} \\ \vdots & \ddots & \vdots \\ c_{(N-1)S_{sub}+F_0,0} & \cdots & c_{(N-1)S_{sub}+F_{M-1},(M-1)S_{sym}} \end{pmatrix}. \quad (1)$$

The received symbol RE at the k -th RE in the m -th RS symbol is represented as [5]:

$$(\mathbf{F}_{Rx})_{k,m} = (\mathbf{F}_{Tx})_{k,m} \cdot \sum_{h=0}^{H-1} (\alpha_h \cdot e^{-\frac{j2\pi k S_{sub} \tau_h}{T_s}} \cdot e^{j2\pi m S_{sym} T f_h}) + (\mathbf{N})_{k,m} \quad (2)$$

Where $(\mathbf{F}_{Tx})_{k,m} = c_{kS_{sub}+F_m, mS_{sym}}$, α_h denotes the complex amplitude of the h -th target, τ_h is the delay of the h -th target, f_h is the Doppler frequency of the h -th target, H is the total number of targets, T_s is the effective OFDM symbol length (inverse of subcarrier spacing (SCS)), T is the total OFDM symbol duration (T_s plus cyclic prefix (CP)), and \mathbf{N} is the matrix of white noise. The post-FFT sensing algorithms operate on received REs by dividing \mathbf{F}_{Rx} by \mathbf{F}_{Tx} elementwise to remove signal modulation. The received RE at the k -th RE in the l -th RS symbol for sensing algorithm processing is thus represented by

$$(\mathbf{F})_{k,m} = \frac{(\mathbf{F}_{Rx})_{k,m}}{(\mathbf{F}_{Tx})_{k,m}} = \sum_{h=0}^{H-1} (\alpha_h \cdot e^{-\frac{j2\pi k S_{sub} \tau_h}{T_s}} \cdot e^{j2\pi m S_{sym} T f_h}) + (\mathbf{N})_{k,m}/(\mathbf{F}_{Tx})_{k,m}. \quad (3)$$

For 2D MUSIC or 2D IAA [10,12], in one snapshot, we vectorize the matrix \mathbf{F} to $\mathbf{A} = \text{vec}(\mathbf{F})$. Let \mathbf{S} be the amplitude vector, and \mathbf{W} be the steering matrix we want to estimate (does not change over snapshots), we write $\mathbf{A} = \mathbf{W}\mathbf{S} + \mathbf{N}'$, where \mathbf{N}' is the vectorized noise $\mathbf{N}' = \text{vec}(\mathbf{N})$, $\mathbf{S} = [\alpha_0 \cdots \alpha_{H-1}]^T$. The h -th column of the steering matrix \mathbf{W} can be written as:

$$\mathbf{w}_{h1}(f_h, \tau_h) = \begin{bmatrix} e^{-\frac{j2\pi(0 \cdot S_{sub} + F_0)\tau_h}{T_s}} e^{j2\pi 0 \cdot S_{sym} T f_h} \\ e^{-\frac{j2\pi(S_{sub} + F_0)\tau_h}{T_s}} e^{j2\pi 0 \cdot S_{sym} T f_h} \\ \vdots \\ e^{-\frac{j2\pi((N-1) \cdot S_{sub} + F_0)\tau_h}{T_s}} e^{j2\pi 0 \cdot S_{sym} T f_h} \\ \vdots \\ e^{-\frac{j2\pi(0 \cdot S_{sub} + F_{M-1})\tau_h}{T_s}} e^{j2\pi(M-1) \cdot S_{sym} T f_h} \\ e^{-\frac{j2\pi(S_{sub} + F_{M-1})\tau_h}{T_s}} e^{j2\pi(M-1) \cdot S_{sym} T f_h} \\ \vdots \\ e^{-\frac{j2\pi((N-1) \cdot S_{sub} + F_{M-1})\tau_h}{T_s}} e^{j2\pi(M-1) \cdot S_{sym} T f_h} \end{bmatrix}. \quad (4)$$

The ambiguities due to aliasing happen when $\mathbf{w}_{h1}(f, \tau) = \mathbf{w}_{h1}(f', \tau')$ and $(f, \tau) \neq (f', \tau')$. We will discuss several cases of RS patterns and the ambiguity performances next.

B. RS Patterns with no staggering offsets

If F_m is constant for any m -th RS symbol, ambiguities happen when

$$e^{-j\left(\frac{2\pi(kS_{sub})}{T_s}\tau'\right)} e^{j2\pi m \cdot S_{sym} T f'} = e^{-j\left(\frac{2\pi(kS_{sub})}{T_s}\tau\right)} e^{j2\pi m \cdot S_{sym} T f}, \quad (5)$$

for all $k = 0, 1, \dots, N-1, m = 0, 1, \dots, M-1$. From Eq. (5), the condition is equivalent to $\tau' = \tau + k_1 T_s / S_{sub}$ and $f' = f + k_2 / (S_{sym} T)$, where τ and f are true delay and Doppler, respectively, and (k_1, k_2) are arbitrary integer pairs. Fig. 2(a) presents the ambiguity performance of 2D MUSIC or IAA with (0,0) as the true delay and Doppler pair in the case of $S_{sym} = 1, S_{sub} = 4$, under 15kHz SCS without staggering. The maximum unambiguous delay is always restricted to T_s / S_{sub} . Fig. 2(b) shows the ambiguity performance of $S_{sym} = 2, S_{sub} = 4$, under 15kHz SCS without staggering.

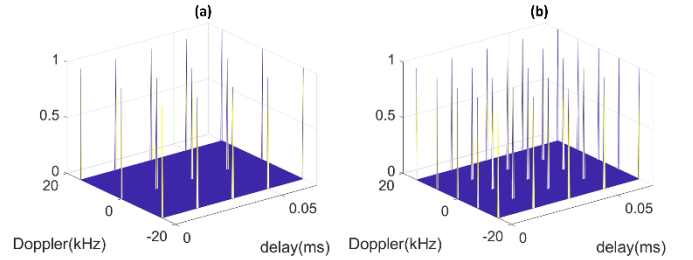


Figure 2. Ambiguity performance with no staggering offsets.

C. Staggering Scheme A

Staggering Scheme A is defined as a linear-slope staggering offset such that $F_m = \text{mod}(p \cdot m + \beta_1, S_{sub})$, where p is relatively prime to S_{sub} and $\beta_1 \in \{0, 1, \dots, S_{sub} - 1\}$, for $m = 0, \dots, M-1$. The ambiguities happen when

$$e^{-j\left(\frac{2\pi(kS_{sub}+mp)}{T_s}\tau'\right)} e^{j2\pi m \cdot S_{sym} T f'} = e^{-j\left(\frac{2\pi(kS_{sub}+mp)}{T_s}\tau\right)} e^{j2\pi m \cdot S_{sym} T f}, \quad (6)$$

for all $k = 0, 1, \dots, N-1$, and all $m = 0, 1, \dots, M-1$.

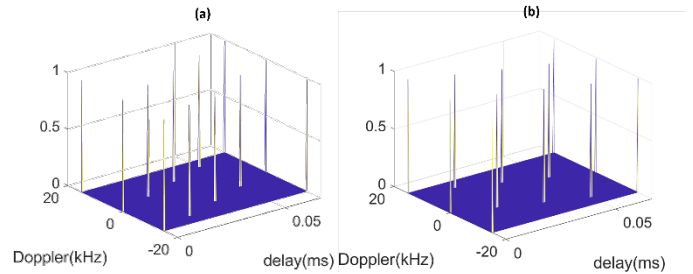


Figure 3. Ambiguity performance with staggering scheme A.

From Eq. (6), we can conclude that the ambiguities happen at $\tau' = \tau + \frac{k_1 T_s}{S_{sub}}$, and $f' = f + \frac{k_2}{S_{sym} T} + \frac{pk_1}{S_{sub} S_{sym} T}$, where (k_1, k_2) are integers and τ and f are true delay and Doppler. Fig. 3 presents ambiguity performance with (0,0) as the true delay and Doppler pair using 2D MUSIC/IAA in the case of $S_{sym} = 1, S_{sub} = 4$ with the staggering scheme A where Fig. 3(a) and 3(b) show the result of $p = 1$ and $p = 3$, respectively.

D. Staggering Scheme B

Note that the steering matrix \mathbf{W} cannot distinguish (τ, f) and $(\tau', f') = (\tau + k_1 T_s, f + k_2 / S_{\text{sym}} T)$ for any integer pair (k_1, k_2) , regardless of choices of staggering offsets. For the staggering Scheme B, it is desirable to have ambiguities only at those (τ', f') values, meaning no side peaks within the best achievable range of time delay (0 to T_s) and Doppler (0 to $1/S_{\text{sym}} T$). This condition for side-peak non-existence can be met if and only if the following statement is true: there are no scalars $\tau' - \tau \in (0, T_s)$ and $f' - f \in \mathbb{R}$ such that the following equation can hold (hereafter referred as “the anti-condition”):

$$e^{-j\left(\frac{2\pi(k S_{\text{sub}} + F_m)}{T_s}\tau'\right)} e^{j2\pi m S_{\text{sym}} T f'} = e^{-j\left(\frac{2\pi(k S_{\text{sub}} + F_m)}{T_s}\tau\right)} e^{j2\pi m S_{\text{sym}} T f}, \quad (7)$$

for all $k = 0, 1, \dots, N-1, m = 0, 1, \dots, M-1$. It can be equivalently re-written into the following form:

$$m \cdot S_{\text{sym}} T (f' - f) - (k \cdot S_{\text{sub}} + F_m) (\tau' - \tau) / T_s = \kappa'_1, \quad (8)$$

where κ'_1 is an arbitrary integer. Since the algorithm is invariant to constant phase rotation, any constant shift $\{F_m + \beta_2\}, \beta_2 \in \mathbb{Z}$ is equivalent to $\{F_m\}$.

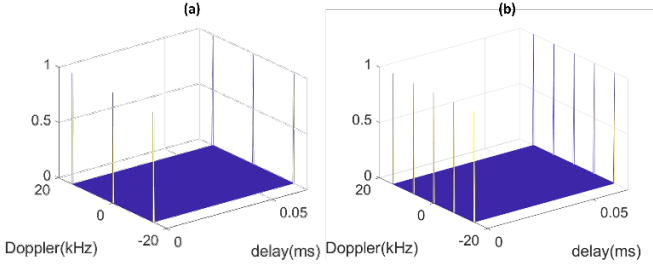


Figure 4. Ambiguity performance with staggering scheme B.

Without loss of generality, we set $F_0 = 0$. Then, for $m = 0$, Eq. (8) gives $(\tau' - \tau) = \kappa_1 T_s / S_{\text{sub}}$. For $\tau' - \tau \in (0, T_s)$, κ_1 must fall within $\{1, 2, \dots, S_{\text{sub}} - 1\}$. Consider $m \neq 0$ and plug in $(\tau' - \tau) = \kappa_1 T_s / S_{\text{sub}}$, Eq. (8) becomes $m \cdot S_{\text{sym}} T (f' - f) - (k \cdot S_{\text{sub}} + F_m) \kappa_1 / S_{\text{sub}}$ and still needs to be an integer. Therefore $m \cdot S_{\text{sym}} T (f' - f) - F_m \kappa_1 / S_{\text{sub}}$ also to be an integer. Thus, the condition is equivalent to lack of a solution $(f' - f, \kappa_1)$ to the equation system

$$\text{mod}(m \cdot S_{\text{sym}} S_{\text{sub}} T (f' - f) - F_m \kappa_1, S_{\text{sub}}) = 0, \quad (9)$$

for $m = 0, 1, \dots, M-1$. Note that should a solution exist, the equation for $m = 1$ implies $S_{\text{sym}} S_{\text{sub}} T (f' - f)$ is an integer, denoted as κ_2 . When $F_0 = 0$, the condition is finally equivalent to no integer solutions $(\kappa_1 \in \{1, 2, \dots, S_{\text{sub}} - 1\}, \kappa_2 \in \mathbb{Z})$ to the equation system

$$\text{mod}(m \kappa_2 - F_m \kappa_1, S_{\text{sub}}) = 0, \quad (10)$$

for $m = 0, 1, \dots, M-1$. In general, for $F_0 \neq 0$, it becomes

$$\text{mod}(m \kappa_2 - (F_m - F_0) \kappa_1, S_{\text{sub}}) = 0, \quad (11)$$

for all $m = 0, 1, \dots, M-1$. When S_{sub} is prime, the only $\{F_m\}$ where Eq. (11) cannot hold is Staggering Scheme A described above. Otherwise, desirable staggering schemes based on the anti-condition can be constructed. The design criteria for Staggering Scheme B are concluded as follows: For a staggering offset sequence $\{F_m\}_{m=0}^{M-1}$, there must not exist a pair of integers (κ_1, κ_2) , where $(\kappa_1 \in \{1, 2, \dots, S_{\text{sub}} - 1\}, \kappa_2 \in \mathbb{Z})$, that can satisfy the modulo equation system in Eq. (11). When the number of equations M is less than or equal to 2, the anti-condition can

always be satisfied by $\kappa_2 = (F_1 - F_0) \kappa_1$. Therefore, $M \geq 3$ is a necessary condition to guarantee non-existence of a solution to the equation system. For instance, 5G PRS satisfies the anti-condition. The example of $(M = 3, S_{\text{sub}} = 4, \{F_i\} = \{0, 3, 1\})$ ambiguity performance is given in Fig. 4(a), and another example of $S_{\text{sub}} = 4, S_{\text{sym}} = 2$ with Staggering Scheme B is given in Fig. 4(b), respectively. High-resolution algorithms such as MUSIC or IAA only need a subset of the staggering cycle to eliminate ambiguity side peaks to achieve the best performance.

III. SYNTHESIS OF REFERENCE SIGNAL

The synthesized RS pattern is shown in Fig. 5, where different colors denote different RSs. The orange RS pattern is the comb RS pattern with uniform symbol spacing (e.g., $S_{\text{sub}} = 4, S_{\text{sym}} = 3, \{F_0, F_1, F_2, F_3\} = \{0, 1, 2, 3\}$ and $M = 4$). Dark blue color denotes a PTRS-like pattern. Let C_1 (unit in subcarrier numbers) be the RE offset of the PTRS-like pattern (i.e., $C_1 = 6$ in Fig. 5), C_2 (unit in symbol numbers) be the time-domain location of the first PTRS-like symbol (i.e., $C_2 = 1$ in Fig. 5), S_F (unit in subcarrier numbers) be the frequency-domain spacing of the PTRS-like REs, S_{PT} (unit in symbol numbers) be the time separation of the PTRS-like symbols (i.e., $S_F = 4, S_{PT} = 3$ in Fig. 5), U_F be the number of frequency-domain REs for one PTRS-like symbol within one snapshot (i.e., $U_F = 2$ in Fig. 5), and U be the number of PTRS-like symbols within one snapshot (i.e., $U = 3$ in Fig. 5). The h -th column of the steering matrix (formed by MUSIC or IAA) can be written as:

$$\mathbf{w}_h(f_h, \tau_h) = \begin{bmatrix} \mathbf{w}_{h1}(f_h, \tau_h) \\ \mathbf{w}_{h2}(f_h, \tau_h) \end{bmatrix}, \quad (12)$$

where $\mathbf{w}_{h1}(f_h, \tau_h)$ is presented in Eq. (4) and

$$\mathbf{w}_{h2}(f_h, \tau_h) = \begin{bmatrix} e^{-\frac{j(2\pi C_1 \tau_h)}{T_s}} e^{j2\pi(C_2 + 0 S_{PT}) T f_h} \\ e^{-\frac{j(2\pi(C_1 + S_F) \tau_h)}{T_s}} e^{j2\pi(C_2 + 0 S_{PT}) T f_h} \\ \vdots \\ e^{-\frac{j(2\pi(C_1 + (U_F - 1) S_F) \tau_h)}{T_s}} e^{j2\pi(C_2 + 0 S_{PT}) T f_h} \\ \vdots \\ e^{-\frac{j(2\pi C_1 \tau_h)}{T_s}} e^{j2\pi(C_2 + (U - 1) S_{PT}) T f_h} \\ e^{-\frac{j(2\pi(C_1 + S_F) \tau_h)}{T_s}} e^{j2\pi(C_2 + (U - 1) S_{PT}) T f_h} \\ \vdots \\ e^{-\frac{j(2\pi(C_1 + (U_F - 1) S_F) \tau_h)}{T_s}} e^{j2\pi(C_2 + (U - 1) S_{PT}) T f_h} \end{bmatrix}. \quad (13)$$

For $\mathbf{w}_{h2} = \emptyset$, analysis was given in the previous section. The best ambiguity performance is limited by \mathbf{w}_{h1} not being unable to distinguish $(\tau' = \tau + k_1 T_s, f' = f + k_2 / (S_{\text{sym}} T))$ for integer pair (k_1, k_2) from (τ, f) . Now after combining with the \mathbf{w}_{h2} , the scheme can remove aliasing (or side peaks with equal power to the main lobe) between (τ, f) and $(\tau' = \tau + k_1 T_s, f' = f + k_2 / T)$ for integer pair (k_1, k_2) . Thus, the ambiguity performance can be future improved with less required RS resources. Now we consider non-empty \mathbf{w}_{h2} . If the vector \mathbf{w}_{h1} is empty, \mathbf{w}_{h2} is equivalent to non-staggered patterns, which cannot eliminate all side peaks. Therefore, we shall focus on the case of $M \geq 1$. We assume that $F_0 = 0$ without loss of generality. At the end of this section, we will apply the phase rotation back and deal with the general case. In such a situation, the pair

(τ, f) cannot be distinguished from the pair (τ', f') using the information from \mathbf{w}_{h2} if the following condition holds true:

$$e^{2\pi j(C_2 + iS_{PT})Tf - 2\pi j \frac{(C_1 + lS_F)}{T_s} \tau} = e^{2\pi j(C_2 + iS_{PT})Tf' - 2\pi j \frac{(C_1 + lS_F)}{T_s} \tau'}, \quad (14)$$

for $i = 0, 1, \dots, U-1, l = 0, 1, \dots, U_F-1$. In the following we consider four cases.

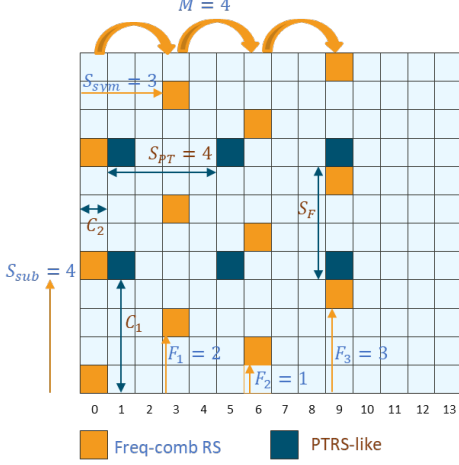


Figure 5. Synthesized RS pattern.

A. Resolving Ambiguities by RE Insertion between 2 Freq-Comb Staggering RS Symbols

In this subsection, we assume $M \geq 2$. Recall that in section II. D, we have shown that to make (τ, f) indistinguishable from the pair (τ', f') , we need $\kappa_1 := (\tau' - \tau)S_{sub}/T_s$ and $\kappa_2 := S_{sym}S_{sub}T(f' - f)$ to be both integers, and the best staggering offset design of the vector \mathbf{w}_{h1} has been shown to be equivalent to Eq. (11). By substituting the expressions of κ_1 and κ_2 in Eq. (11) into Eq. (14), we get an additional anti-condition.

$$\text{mod}((C_2 + iS_{PT})\kappa_2 - (C_1 + lS_F)S_{sym}\kappa_1, S_{sym}S_{sub}) = 0, \quad (15)$$

for any $i = 0, 1, \dots, U-1, l = 0, 1, \dots, U_F-1$. Above derivations assume $F_0 = 0$. In general, one may replace C_1 with $C_1 - F_0$, and F_m with $F_m - F_0$ and obtain the general rules for combining staggering frequency comb RS with a PTRS-like pattern: neither the condition in Eq. (11) nor the following anti-condition of PTRS-like pattern

$$\text{mod}((C_2 + iS_{PT})\kappa_2 - (C_1 + lS_F - F_0)S_{sym}\kappa_1, S_{sym}S_{sub}) = 0, \quad (16)$$

holds true for $i = 0, 1, \dots, U-1, l = 0, 1, \dots, U_F-1$. Then the ambiguity due to aliasing does not exist in desired ranges of delay $\tau \in (0, T_s)$ and Doppler $f \in (0, 1/T)$. Case 1 in Fig. 6 shows a frequency staggering comb RS with $M = 2, F_0 = 0$ and $F_1 = 1$. One way of ensuring the nonexistence of the solution is by taking $U \geq 1$, and choosing the pair (C_1, C_2) such that $C_2 + iS_{PT} - (C_1 + lS_F - F_0)S_{sym}$ and $S_{sym}S_{sub}$ are relatively prime for some $i^* \in \{0, 1, \dots, U-1\}$ and $l^* \in \{0, 1, \dots, U_F-1\}$. In such case, first anti-condition Eq. (11) implies that $\kappa_2 - \kappa_1$ is an integer multiple of S_{sub} , implying $\text{mod}((C_1 + lS_F - F_0)S_{sym}(\kappa_1 - \kappa_2), S_{sym}S_{sub}) = 0$. By substituting the above into the anti-condition Eq. (16), we have $\text{mod}((C_2 + iS_{PT} - (C_1 + lS_F - F_0)S_{sym})\kappa_2, S_{sym}S_{sub}) = 0$. Since $C_2 + iS_{PT} - (C_1 + lS_F - F_0)S_{sym}$ and $S_{sym}S_{sub}$ are

relatively prime for some $i^* \in \{0, 1, \dots, U-1\}$ and $l^* \in \{0, 1, \dots, U_F-1\}$, the anti-condition at the pair (l^*, i^*) requires κ_2 to be an integer multiple of $S_{sym}S_{sub}$, implying κ_1 is an integer multiple of S_{sub} . Since we have $\kappa_1 \in \{0, 1, \dots, S_{sub}-1\}$ and $\kappa_2 \in \{0, 1, \dots, S_{sym}S_{sub}-1\}$, the only possibility is $\kappa_1 = \kappa_2 = 0$. Therefore, the combined RS pattern requirement is: on top of 2 staggering freq-comb RS symbols, adding a PTRS-like RS with $U \geq 1$ and/or $U_F \geq 1$, if $C_2 + i^*S_{PT} - (C_1 + l^*S_F - F_0)S_{sym}$ and $S_{sym}S_{sub}$ are relatively prime for some $i^* \in \{0, 1, \dots, U-1\}$ and $l^* \in \{0, 1, \dots, U_F-1\}$, then ambiguity due to aliasing does not exist in the desired range. An example of the PTRS pattern parameters (U, U_F, C_1, C_2) are given in Fig. 6.

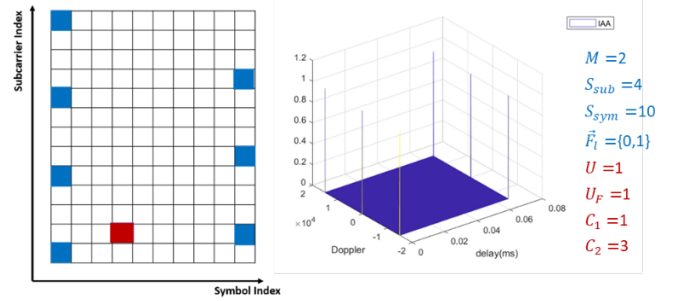


Figure 6. Examples of Case 1

B. Resolving Ambiguities by Combining PTRS with Single Freq-Comb PRS

This case assumes $M = 1, U \geq 2$ and $U_F = 1$. Comparing the cases $(i = 0, l = 0)$ and $(i = 1, l = 0)$ for Eq (14) implies that ambiguity arises in \mathbf{w}_{h2} if the quantity $\kappa_3 = S_{PT}T(f' - f)$ is an integer in $\{0, 1, \dots, S_{PT}-1\}$. Additionally, the indistinguishability of the vector \mathbf{w}_{h1} in the $i = 0$ case requires that $\kappa_1 := (\tau' - \tau)S_{sub}/T_s$ is an integer in $\{0, 1, \dots, S_{sub}-1\}$. Furthermore, applying Eq (14) with $(i = 0, l = 0)$ implies ambiguity if the term $C_2T(f' - f) - \frac{C_1}{T_s}(\tau' - \tau) = \frac{C_2}{S_{PT}}\kappa_3 - \frac{C_1}{S_{sub}}\kappa_1$ is an integer. On the other hand, if $\kappa_1, \kappa_3, \frac{C_2}{S_{PT}}\kappa_3 - \frac{C_1}{S_{sub}}\kappa_1$ are all integers, then $(C_2 + iS_{PT})T(f' - f) - \frac{C_1}{T_s}(\tau' - \tau) = \frac{C_2}{S_{PT}}\kappa_3 - \frac{C_1}{S_{sub}}\kappa_1 + l\kappa_3$ is an integer and the anti-condition Eq. (14) will hold for any $i \geq 0$. Therefore, for a single freq-comb symbol's ambiguities to be resolved by a PTRS-tone ($U \geq 2, U_F = 1$), non-existence of any non-zero pair solution, $(\kappa_1, \kappa_3) \in [0, S_{sub}-1] \times [0, S_{PT}-1]$, to the following anti-condition:

$$\frac{C_2}{S_{PT}}\kappa_3 - \frac{C_1 - F_0}{S_{sub}}\kappa_1 \in \mathbb{Z} \quad (17)$$

must be satisfied. Case 2 in Fig. 7 illustrates such a synthesized RS scheme with the right combinations of comb-RS and PTRS parameters $(M, S_{sub}, U, U_F, C_1, C_2)$.

Another design is based on $M = 1, U \geq 2$ and $U_F \geq 2$, as illustrated in Fig. 8. In addition to ambiguity analysis in Case 2, $\frac{S_F}{T_s}(\tau' - \tau) = \frac{S_F}{S_{sub}}\kappa_1$ being an integer creates ambiguity as Eq. (14) in the cases of $(i = 0, l = 1)$ and $(i = 0, l = 0)$. If $\kappa_1, \kappa_3, \frac{C_2}{S_{PT}}\kappa_3 - \frac{C_1}{S_{sub}}\kappa_1, \frac{S_F}{S_{sub}}\kappa_1$ are all integers, we have that

$$(C_2 + i S_{PT})T(f' - f) - \frac{C_1 + i S_F}{T_s}(\tau' - \tau) = \frac{C_2}{S_{PT}}\kappa_3 - \frac{C_1}{S_{sub}}\kappa_1 + i\kappa_3 - \frac{S_F}{S_{sub}}\kappa_3 \in \mathbb{Z}. \quad (18)$$

and the anti-condition Eq (14) will hold for any $l \geq 0$ and $i \geq 0$. Therefore, for a single freq-comb symbol's ambiguities to be resolved by two or more PTRS tones ($U \geq 2$, $U_F \geq 2$), non-existence of any non-zero pair solution to either of the following anti-condition:

$$\frac{C_2}{S_{PT}}\kappa_3 - \frac{C_1 - F_0}{S_{sub}}\kappa_1 \in \mathbb{Z}, \quad \frac{S_F}{S_{sub}}\kappa_1 \in \mathbb{Z}. \quad (19)$$

must be satisfied for $(\kappa_1, \kappa_3) \in [0, S_{sub} - 1] \times [0, S_{PT} - 1]$. Fig. 8 illustrates an example using IAA.

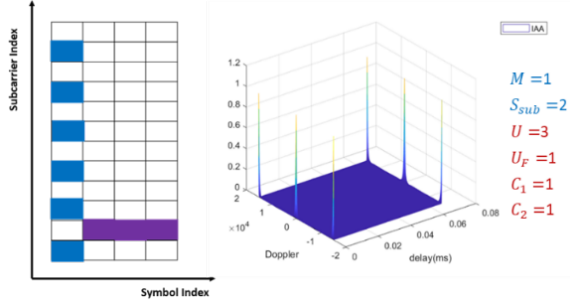


Figure 7. Example of case 2

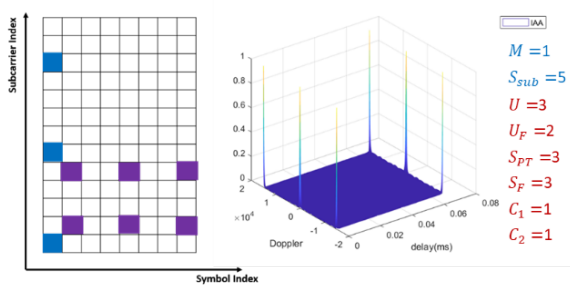


Figure 8. Example of Case 3.

IV. GENERAL IRREGULAR RS PATTERNS

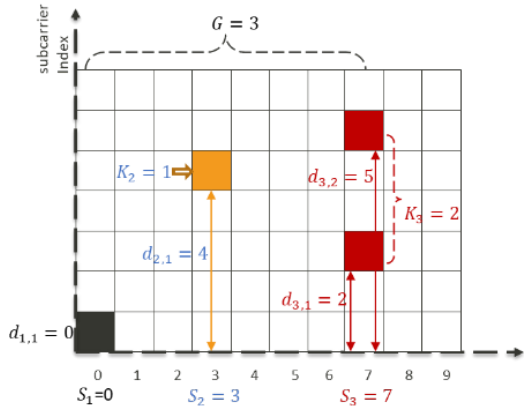


Figure 9 Irregular RS Pattern of Case 4

Now let's turn to a general irregular RS pattern. Denote d_{gj} as RE offset of the j th RE at the g th RS symbol, K_g as the total number of RS REs at the g th RS symbol, S_g as the RS symbol index of the g th RS symbol, and G as the total number of RS symbols. A graphical illustration is given in Fig. 10. Note that d_{ij} and S_g are not necessarily uniform spaced, which could

form an irregular pattern. The h -th column of the steering matrix is therefore listed below:

$$\mathbf{w}_h'(f_h, \tau_h) = \begin{bmatrix} e^{-\frac{j(2\pi d_{11}\tau_h)}{T_s}} e^{j2\pi S_1 T f_h} \\ e^{-\frac{j(2\pi d_{12}\tau_h)}{T_s}} e^{j2\pi S_1 T f_h} \\ \vdots \\ e^{-\frac{j(2\pi d_{1K_1}\tau_h)}{T_s}} e^{j2\pi S_1 T f_h} \\ e^{-\frac{j(2\pi d_{21}\tau_h)}{T_s}} e^{j2\pi S_2 T f_h} \\ e^{-\frac{j(2\pi d_{22}\tau_h)}{T_s}} e^{j2\pi S_2 T f_h} \\ \vdots \\ e^{-\frac{j(2\pi d_{2K_2}\tau_h)}{T_s}} e^{j2\pi S_2 T f_h} \\ \vdots \\ e^{-\frac{j(2\pi d_{G1}\tau_h)}{T_s}} e^{j2\pi S_G T f_h} \\ e^{-\frac{j(2\pi d_{G2}\tau_h)}{T_s}} e^{j2\pi S_G T f_h} \\ \vdots \\ e^{-\frac{j(2\pi d_{GK_G}\tau_h)}{T_s}} e^{j2\pi S_G T f_h} \end{bmatrix}, \quad (20)$$

A pair of parameters (τ, f) results in ambiguity with another pair (τ', f') , if for any $g \in \{1, 2, \dots, G\}$ and $k \in \{1, 2, \dots, K_g\}$,

$$\Phi(g, k) = (S_g - S_1)T(f' - f) - (d_{gk} - d_{11})\frac{\tau' - \tau}{T_s} \in \mathbb{Z}. \quad (21)$$

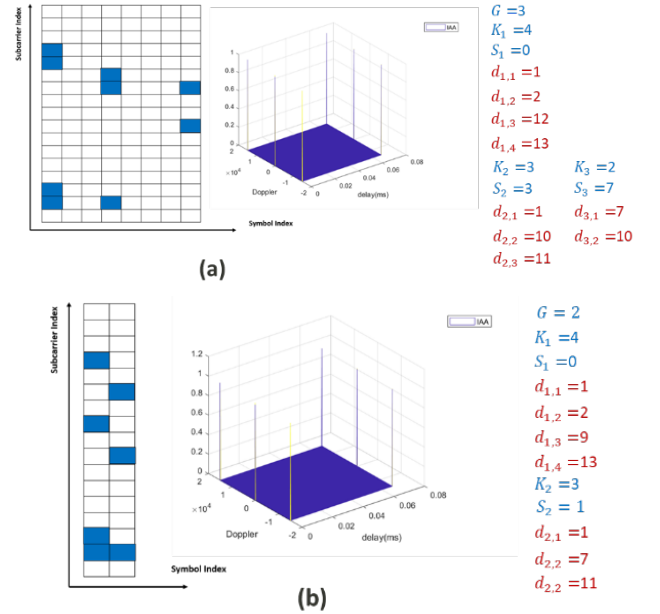


Figure 10. Examples of Case 4.

A. Two or more REs for at least One RS symbol

There exists a $g^* \in \{1, 2, \dots, G\}$, such that $K_{g^*} \geq 2$. Take an arbitrary distinct pair $(k^*, l^*) \in \{1, \dots, K_{g^*}\} \times \{1, \dots, K_{g^*}\}$, where $k^* \neq l^*$. And define $d^* := \min_{g: K_g \geq 2} \min_{k \neq l} |d_{gk} - d_{gl}|$. Due to invariance to constant phase rotation, we can assume $d_{11} = S_1 = 0$ without loss of generality. Applying Eq. (21) with (g^*, k^*) and (g^*, l^*) and taking their difference, we have that $\kappa_1 := d^* \frac{\tau' - \tau}{T_s} \in \mathbb{Z}$. If an ambiguity exists in the range $\tau' - \tau \in [0, T_s]$, we have that $\kappa_1 \in \{0, 1, 2, \dots, d^* - 1\}$. Substituting into Eq (21), we have that

$$S_g T(f' - f) - \frac{d_{gk}}{d^*} \kappa_1 \in \mathbb{Z}, \quad (22)$$

for any $g \in \{1, 2, \dots, G\}$ and $k \in \{1, 2, \dots, K_g\}$. Consequently, we have $d^* S_g T(f' - f) \in \mathbb{Z}$. Since we have assumed $S_1 = 0$, we need $G \geq 2$ and $S_2 \neq 0$ for this constraint to be effective. Let $S^* := \gcd(S_2 - S_1, \dots, S_G - S_1)$, where \gcd denotes the greatest common divisor. We have $\kappa_2 := S^* d^* T(f' - f) \in \mathbb{Z}$. If $f' - f \in [0, 1/T]$, we have $\kappa_2 \in \{0, 1, 2, \dots, S^* d^* - 1\}$. Under such a representation, the anti-condition Eq (21) becomes $\text{mod}(S_g \kappa_2 - d_{gk} S^* \kappa_1, S^* d^*) = 0$, for any $g \in \{1, 2, \dots, G\}$ and $k \in \{1, 2, \dots, K_g\}$. Above derivations are based on the assumption $S_1 = d_{11} = 0$. In general, one may replace S_g with $S_g - S_1$, and d_{gk} with $d_{gk} - d_{11}$, and obtain the anti-condition

$$\text{mod}((S_g - S_1)\kappa_2 - (d_{gk} - d_{11})S^* \kappa_1, S^* d^*) = 0, \quad (23)$$

for any $g \in \{1, 2, \dots, G\}$ and $k \in \{1, 2, \dots, K_g\}$. Therefore, the distinguishability in the desirable range $\tau' - \tau \in (0, T_s)$, $f' - f \in (0, 1/T)$ is equivalent to the non-existence of a non-zero solution $\kappa_1 \in \{0, 1, \dots, d^* - 1\}$, $\kappa_2 \in \{0, 1, \dots, S^* d^* - 1\}$ to Eq (23). In this case, we need $G \geq 2$, with at least one RS symbol satisfying $K_g \geq 2$. At least 3 entries are need for the vector \mathbf{w}_h . Fig.10 shows two examples of this case (case 4).

B. Single RE for Every RS symbol

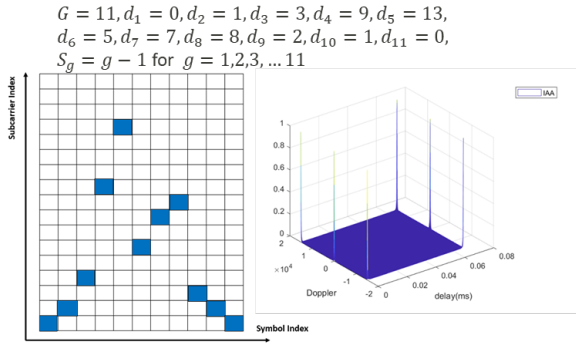


Figure 11. Example of case 5.

The RS pattern is parameterized as: $\forall g \in \{1, 2, \dots, G\}$, $K_g = 1$. For notation simplicity, we use d_g to denote d_{g1} for any $g \in \{1, 2, \dots, G\}$. Following similar derivation from previous section, to avoid all $(d_g - d_1, S_g - S_1)$ integer pairs being integer multiples of an integer pair (\bar{d}, \bar{S}) , there must exist a distinct index pair (m^*, n^*) , where $m^* \geq 2$, $n^* \geq 2$, $m^* \neq n^*$, such that $(d_{m^*} - d_1) / (S_{m^*} - S_1) \neq (d_{n^*} - d_1) / (S_{n^*} - S_1)$. If not, there will be (τ, f) and (τ', f') satisfying $\frac{\tau' - \tau}{T_s} (\bar{d} - d_1) = (\bar{S} - S_1) T(f' - f)$, resulting in ambiguity in Eq. (21). Define $S_{m^*, n^*}^* = |(d_{m^*} - d_1)(S_{n^*} - S_1) - (S_{m^*} - S_1)(d_{n^*} - d_1)|$. Moreover, from Eq. (21), we have $(S_{n^*} - S_1) \times \Phi(m^*, 1) - (S_{m^*} - S_1) \times \Phi(n^*, 1) \in \mathbb{Z}$, one obtains $\kappa_1 := S_{m^*, n^*}^* \frac{\tau' - \tau}{T_s} \in \mathbb{Z}$. On the other hand, $(d_{n^*} - d_1) \times \Phi(m^*, 1) - (d_{m^*} - d_1) \times \Phi(n^*, 1) \in \mathbb{Z}$ yields $\kappa_2 := S_{m^*, n^*}^* T(f' - f) \in \mathbb{Z}$. Substituting κ_1 and κ_2 into Eq. (21), the anti-condition is: there is no non-zero integer pair (κ_1, κ_2) , where $\kappa_1, \kappa_2 \in \{0, 1, \dots, S_{m^*, n^*}^* - 1\}$, such that, for any $g, m^*, n^* \in \{1, 2, \dots, G\}$

$$\text{mod}((S_g - S_1)\kappa_2 - (d_g - d_1)\kappa_1, S_{m^*, n^*}^*) = 0. \quad (24)$$

In this case, we have $G \geq 3$, and at least 3 entries are needed in the vector \mathbf{w}_h . Note that the above only guarantees no side peaks due to aliasing (i.e., side peaks with equal power to mainlobe) in the range $\tau' - \tau \in (0, T_s)$, $f' - f \in (0, 1/T)$. In general, side peaks with lower power than the mainlobe might exist due to the choices of algorithms and RS patterns. In such case, the anti-conditions derived in this paper serve as a constraint in the optimization problem of RS patterns design.

V. CONCLUSION

In this paper, we analyze ambiguity performance of current 5G comb RS pattern and derive general rules for synthesized RS patterns. With proper design of staggering offsets, best achievable ambiguity performance in delay and Doppler domains using high-resolution algorithms is obtained for both uniform spacing comb RSs and general irregular RSs. Based on derived rules, synthesized RS patterns of generalized irregular form further enhance OFDM sensing RS efficiency by preserving its ambiguity performance, yet with reduced system overhead when using high-resolution algorithms.

REFERENCES

- [1] F. Liu, C. Masouros, A. P. Petropulu, H. Griffiths and L. Hanzo, "Joint Radar and Communication Design: Applications, State-of-the-Art, and the Road Ahead," in IEEE Transactions on Communications, vol. 68, no. 6, pp. 3834-3862, June 2020.
- [2] L. Zheng, M. Lops, Y. C. Eldar and X. Wang, "Radar and Communication Coexistence: An Overview: A Review of Recent Methods," in IEEE Signal Processing Magazine, vol. 36, no. 5, pp. 85-99, Sept. 2019
- [3] D. H. N. Nguyen and R. W. Heath, "Delay and Doppler processing for multi-target detection with IEEE 802.11 OFDM signaling," 2017 IEEE International Conference on Acoustics, Speech and Signal Processing.
- [4] P. Kumari, J. Choi, N. González-Prelcic and R. W. Heath, "IEEE 802.11ad-Based Radar: An Approach to Joint Vehicular Communication-Radar System," in IEEE Transactions on Vehicular Technology, vol. 67, no. 4, pp. 3012-3027, April 2018.
- [5] M. Braun, C. Sturm and F. K. Jondral, "Maximum likelihood speed and distance estimation for OFDM radar," 2010 IEEE Radar Conference, Arlington, VA, USA, 2010.
- [6] A. Evers and J. A. Jackson, "Analysis of an LTE waveform for radar applications," 2014 IEEE Radar Conference, Cincinnati, OH, USA, 2014.
- [7] Z. Wei et al., "5G PRS-Based Sensing: A Sensing Reference Signal Approach for Joint Sensing and Communication System," in IEEE Transactions on Vehicular Technology, vol. 72, no. 3, pp. 3250-3263, March 2023.
- [8] Q. Zhao, A. Tang and X. Wang, "Reference Signal Design and Power Optimization for Energy-Efficient 5G V2X Integrated Sensing and Communications," in IEEE Transactions on Green Communications and Networking, vol. 7, no. 1, pp. 379-392, March 2023.
- [9] 3GPP TR38.211 and Chapter 24 of "5G NR: The Next Generation Wireless Access Technology, 2nd edition" by E. Dahlman, et al.
- [10] W. Roberts, P. Stoica, J. Li, T. Yardibi and F. A. Sadjadi, "Iterative Adaptive Approaches to MIMO Radar Imaging," in IEEE Journal of Selected Topics in Signal Processing, vol. 4, no. 1, pp. 5-20, Feb. 2010.
- [11] Hayes, Monson H., Statistical Digital Signal Processing and Modeling, John Wiley & Sons, Inc., 1996.
- [12] F. Belfiori, W. van Rossum and P. Hoogetboom, "Application of 2D MUSIC algorithm to range-azimuth FMCW radar data," 2012 9th European Radar Conference, Amsterdam, Netherlands, 2012, pp. 242-245.